Acta Cardiol Sin 2023;39:580–598
Original Article
doi: 10.6515/ACS.202307_39(4).20221219B

Basic Science/Heart Failure

Analysis of Fatty Acid Metabolism in Fetal and Failing Hearts by Single-Cell RNA Sequencing Revealed *SLC27A6* as a Critical Gene in Heart Maturation

Wenjia Zhu,[1†] Yufan Zheng,[1†] Jiaying Liu,[1] Chao Zhao,[1] Ning Sun,[1,2#] Xiuxia Qu[2#] and Hui Yang[1,2]

Background: Heart failure is associated with shifts in substrate preferences and energy insufficiency. Although cardiac metabolism has been explored at the organ level, the metabolic changes at the individual cell level remain unclear. This study employed single-cell ribonucleic acid (RNA) sequencing to investigate the cell-type-specific characteristics of gene expression related to fatty acid metabolism.

Methods: Single-cell RNA sequencing data from fetal hearts were processed to analyze gene expression patterns related to fatty acid metabolism. Immunofluorescence staining and Western blotting techniques were employed to validate the expression of specific proteins. Additionally, calcium recording and contractility measurements were performed to assess the functional implications of fatty acid metabolism in cardiomyocytes.

Results: Based on single-cell RNA sequencing data analysis, we found that a decrease in overall energy requirements underlies the downregulation of fatty acid oxidation-related genes in the later period of heart maturation and the compensatory increase of fatty acid metabolism in individual cardiomyocytes during heart failure. Furthermore, we found that solute carrier family 27 member 6 (SLC27A6), a fatty acid transport protein, is involved in cardiac maturation. SLC27A6 knockdown in human induced pluripotent stem cell-derived cardiomyocytes resulted in an immature cardiomyocyte transcriptional profile, abnormal morphology, impaired Ca^{2+} handling activity, and contractility.

Conclusions: Overall, our study offers a novel perspective for exploring cardiac fatty acid metabolism in fetal and failing hearts along with new insights into the cellular mechanism underlying fatty acid metabolic alterations in individual cardiac cells. It thus facilitates further exploration of cardiac physiology and pathology.

Key Words: Cardiac maturation • Fatty acid metabolism • Heart failure • Single-cell sequencing analysis • *SLC27A6*

INTRODUCTION

In the mammalian body, the heart contracts continuously to supply blood to all organs and tissues. In a healthy adult heart, oxidation of long-chain fatty acids (LCFAs) is preferred for adenosine triphosphate (ATP) production to satisfy its high energy requirements,[1] and approximately 40-70% of the total ATP is provided through fatty acid (FA) β-oxidation.[2] Adaptive changes in cardiac energy metabolism have been reported under various physiological and pathological conditions. Heart failure (HF) is associated with a shift in energy substrate preference, impaired mitochondrial oxidative phosphorylation,[2,3] energy insufficiency[4] and oxidative stress.[5] The fetal heart utilizes carbohydrates as its major energy source during gestation,[6] and FAs contribute to less than 15% of the to-

Received: April 5, 2022 Accepted: December 19, 2022
[1]Department of Physiology and Pathophysiology, State Key Laboratory of Medical Neurobiology, School of Basic Medical Sciences, Fudan University, Shanghai; [2]Wuxi School of Medicine, Jiangnan University, Jiangsu, China.
Corresponding author: Dr. Hui Yang, School of Basic Medical Sciences, Fudan University, Shanghai, 200032, China. E-mail: yanghuiyh@fudan.edu.cn
[#] Sun and Qu contributed equally as corresponding authors to this paper.
[†] Zhu and Zheng contributed equally to this paper.

Abbreviations

ACS	Acyl-CoA synthase
ACSM3	Acyl-CoA synthetase medium chain family member 3
ATP	Adenosine triphosphate
AV	Atrial and ventricular
CD36	CD36 molecule
CM	Cardiomyocyte
cTnT	Cardiac troponin T (protein)
FA	Fatty acid
FABP3	Fatty acid binding protein 3
FABP4	Fatty acid binding protein 4
FATP	Fatty acid transport protein
hESC	Human embryonic stem cell
HF	Heart failure
hiPSC	Human induced pluripotent stem cell
KD	*SLC27A6* knockdown
KEGG	Kyoto Encyclopedia of Genes and Genomes
LCFA	Long-chain fatty acid
LPL	Lipoprotein lipase
mRNA	Messenger ribonucleic acid
MYH7	Myosin heavy chain 7
MYL2	Myosin light chain 2
MYL7	Myosin light chain 7
NC	Negative control
NGS	Next-generation sequencing
PCR	Polymerase chain reaction
PPAR	Peroxisome proliferator activated receptor
PVDF	Polyvinylidene fluoride
RNA	Ribonucleic acid
scRNA-seq	Single-cell RNA sequencing
shRNA	Short hairpin ribonucleic acid
SLC27A	Solute carrier 27A
SLC27A6	Solute carrier family 27 member 6
UMAP	Uniform manifold approximation and projection

tal myocardial ATP production via β-oxidation.[7]

In mammalian embryos, heart maturation is accompanied by a transition from fetal metabolism to adult metabolism,[8] and the switch in energy substrate preference from carbohydrates to FAs has been confirmed to be a central driver of cardiac maturation.[9] High glucose treatment maintains human embryonic stem cell-derived cardiomyocytes and human induced pluripotent stem cell-derived cardiomyocytes (hiPSC-CMs) by promoting aerobic glycolysis and nucleotide biosynthesis, whereas glucose reduction enhances maturation.[10-12] Conversely, supplementation with FAs has been shown to promote the maturation of hiPSC-CMs, resulting in increased adult metabolism in parallel with morphologically and functionally advanced phenotypes.[13-16] Activation of peroxisome proliferator activated receptor α (PPARα) has also been reported to exert pro-maturation effects on cardiomyocytes (CMs) by augmenting the expression levels of enzymes associated with FA oxidation,[17,18] indicating a strong link between cardiac metabolism and maturation.

LCFAs are taken up into the cytoplasm through a protein-mediated transport system. Fatty acid transport proteins (FATPs) are transmembrane proteins that function as LCFA transporters[19,20] as well as acyl-CoA synthases (ACSs), which convert FAs to acyl-CoA thioesters.[19,21,22] The solute carrier 27A (SLC27A) gene family encodes six highly homologous FATPs.[21,23] Encoded by solute carrier family 27 member 6 (*SLC27A6*), FATP6/SLC27A6 is the predominant isoform expressed in the heart and is responsible for LCFA translocation across the CM membrane.[21,24] Previous research has reported that variations in *SLC27A6* are associated with reduced triglyceride levels, blood pressure, and left ventricular hypertrophy *in vivo*.[25] In hiPSC-CMs, *SLC27A6* knockdown results in hypertrophic phenotypes.[26]

Over the decades, cardiac metabolism and its interactions with heart maturation, contraction, and heart diseases have been increasingly noted. However, research has mainly focused on organ or tissue levels, and there are few insights into single-cell FA metabolism in the heart. In particular, previous studies have mostly ignored the heterogeneity among different types of cardiac cells. Recent developments in next-generation sequencing have facilitated the exploration of heterogeneity among individual cells.[27] Therefore, we focused on FA metabolism within individual cells in the human heart using single-cell ribonucleic acid (RNA) sequencing (scRNA-seq) analysis in this study. These results will advance our understanding of FA metabolism during cardiac maturation and facilitate further exploration of cardiac physiology.

METHODS

Data acquisition

Three independent scRNA-seq datasets (GSE106118, GSE109816, and GSE121893) were obtained from gene expression omnibus datasets. The GSE106118 dataset contained the scRNA-seq data of 98 human fetal hearts at different timepoints, from which we chose the timepoints of

5 weeks (5 W), 10 W, and 20 W of gestation. The GSE 121893 and GSE109816 datasets contained the single-cell sequencing of human adult hearts with (8 samples) and without HF (12 samples), respectively. As the causes of HF in these patients were different, we grouped the patients as dHF (caused by dilated cardiomyopathy) and cHF (caused by coronary heart disease) groups. We processed these data using the Seurat package in R (version 4.0.4).

Quality control, data normalization, and cell clustering

In R, the CreateSeuratObject package was used to create Seurat objects with the data, and quality control was performed to filter out cells with improper gene counts, gene features, and proportions of mitochondrial genes. The NormalizeData function was used to normalize the expression matrices of filtered samples. The top 2000 genes with the most variations among cells were selected using the FindVariableFeatures function, and linear dimensionality reduction analysis was performed using the RunPCA function. FindNeighbors and FindClusters functions were used to cluster cells; the Run-uniform manifold approximation and projection (UMAP) function was then used for UMAP to analyze dimension reduction. The FindAllMarkers function was used to identify genes with differential expressions among clusters.

Cell type identification

Using marker gene profiling of the reviewed marker genes[28] and markers from the CellMarker database (http://biocc.hrbmu.edu.cn/CellMarker/),[29] we grouped and defined the cell clusters from these datasets (Supplementary Figure 1A-1D). To define cardiomyocytes, we found a cluster highly expressing ventricular CM marker genes [Myosin heavy chain 7 (MYH7), Myosin light chain 2 (MYL2), and four and a half LIM domains 2 (FHL2)] and a cluster highly expressing atrial CM marker genes [natriuretic peptide A , Myosin light chain 7 (MYL7), and Myosin light chain 4 (MYL4)]. We also found a cluster that expressed ventricular and atrial CM marker genes highly and equally; therefore, we defined it as atrial and ventricular CMs (AV CMs).[30] We performed Kyoto Encyclopedia of Genes and Genomes (KEGG) pathway enrichment analysis for the marker genes of AV CM clusters. The top 20 enriched KEGG pathways are shown in Supplementary Figure 2. The genes highly expressed in AV CMs were enriched in myocardial contraction, the apelin signaling pathway, adrenergic signaling in CMs, and regulation of the actin cytoskeleton.

hiPSC-CM differentiation

hiPSCs were previously reprogrammed in our laboratory.[31] Before differentiation, induced pluripotent stem cell (iPSCs) were seeded on 12-well culture plates coated with 1.5% Matrigel Membrane Matrix (Corning) and maintained in mTeSR-1 medium (Stemcell Technologies). The cells were passaged using Accutase (Sigma) at 75% density and reseeded on a new Matrigel-coated 12-well plate at about 5×10^5 cells/well. When the iPSCs reached 80-90% density, they were treated with 7 μM CHIR99021 (Selleck) in RPMI 1640 medium (Corning) containing 2% B27 Supplement minus insulin (Life Technology) for 3 days. Then, 5 μM IWR-1 (Selleck) was added to RPMI1640 basal medium supplemented with 2% B27 without insulin on days 4-5. From day 5, the cells were cultured with CDM3 medium [RPMI 1640 basal medium containing l-ascorbic acid (Sigma) and Bovine serum albumin (Sigma)], with the medium changed every other day. On days 7-10 post cardiac differentiation, beating cells were observed in the control group. All cultures were maintained at 37 °C with 5% CO_2.

Transduction of *SLC27A6* short hairpin ribonucleic acid (shRNA)

Three candidate shRNA sequences for *SLC27A6* were designed based on the human *SLC27A6* messenger ribonucleic acid (mRNA) sequence (NM_014031.5) and cloned into the pLKO.1-GFP lentiviral vector (Transheep Co., Shanghai, China). Target shRNA plasmids and scrambled shRNA plasmids (Transheep Co., Shanghai, China) were transfected into iPSC-CMs using Lipofectamine 3000 (Thermo Fisher Scientific) to examine their knockdown efficiency. Using real-time polymerase chain reaction (PCR), one shRNA sequence (5′-CCGGCAGCTACCGAATC AAGCATATCTCGAGATATGCTTGATTCGGTAGCTGTTTTTT-3′) was found to be the most effective at suppressing *SLC27A6* mRNA expression in iPSC-CMs. Both the target and scrambled short hairpin ribonucleic acid (shRNA) plasmids were packaged in 293T cells, and the resulting lentivirus-containing medium was added to iPSC-CMs for lentiviral-mediated transduction. Knockdown efficiency was determined using real-time PCR and Western blotting.

Real-time PCR analysis

Total cellular RNA was extracted from hiPSC-CMs using Trizol reagent (Life Technologies), and 1 μg RNA was reverse transcribed using a ReverTra Ace qPCR RT Kit (Vazyme). The resulting cDNA was then used as a template for amplification using SYBR Green Real-time PCR master mix (Vazyme) on a Real-Time System instrument (Roche). Each reaction was performed in triplicate. Measurements were performed using the $2^{-\Delta\Delta Ct}$ method; the housekeeping gene, glyceraldehyde-3-phosphate dehydrogenase, was used as an internal control. The primers used are listed in Table 1.

Immunofluorescence staining

hiPSC-CMs were fixed in 4% paraformaldehyde for 15 min, permeabilized with 0.5% Triton X-100 for 15 min, washed three times, and blocked with goat serum for 30 min at room temperature. The cells were incubated overnight at 4 °C with primary anti-cardiac troponin T (cTnT) antibodies (Abcam). The cells were washed three times and incubated with secondary antibodies (Abcam) at 37 °C for 60 min. Finally, the cells were washed, and the nuclei were stained with DAPI. Images were visualized and captured using a Leica DMi8 confocal microscope (Leica).

Calcium recording and contractility measurement

Cultured hiPSC-CMs at day 28 were dissociated, seeded on a confocal dish, and cultured for another two days in Dulbecco's modified Eagle medium supplemented with 10% fetal bovine serum. For calcium recording, hiPSC-CMs were treated with Cal-520 TM and 0.02% Pluronic F-127 (AAT Bioquest, Sunnyvale, USA) at 37 °C for 20 min and then washed twice with fresh warm medium. The cells were then placed in a microincubation chamber (37 °C, 5% CO_2), and Ca^{2+} transient signals were recorded using an LSM-710 laser scanning confocal microscope (Carl Zeiss) in the XT line-scan mode. MATLAB software (MathWorks) was used to analyze the Ca^{2+} signals. For contractility measurement, a video-based motion edge detection system was used to record the spontaneous contraction traces of hiPSC-CMs; the data were analyzed using FelixGX software.

Western blot

Cells were lysed using a modified radio immunoprecipitation assay solution (Beyotime) containing protease and phosphatase inhibitors (Beyotime) for 30 min at 4 °C. The complex was then centrifuged at 12,000 × *g* for 10 min and the supernatant was collected. To determine the total protein content, the protein supernatant was quantified using a BCA Protein Assay Kit (TIANGEN). Equivalent amounts of protein (20 μg) were separated using a 10% gel and then transferred to a polyvinylidene fluoride (PVDF) membrane (Bio-Rad). The PVDF membranes were then incubated overnight at 4 °C with the anti-SLC 27A6 antibody (SAB) with 10% milk, followed by the secondary antibody for 2 hours at room temperature. High-sig ECL Western blotting Substrate (Tanon) was used to detect the proteins. ImageJ software was used to analyze the Western blot signals.

Statistical analysis

All data are shown as the mean ± standard error of the mean. Two groups of normally distributed data were compared using the Student's t-test. Statistical significance was set at $p < 0.05$ as * $p < 0.05$, ** $p < 0.01$, and *** $p < 0.001$.

RESULTS

Fatty acid metabolism during cardiac development and maturation

We processed scRNA-seq data from the fetal heart

Table 1. Sequence of primers used in real-time PCR

Gene	Forward	Reward
MYH7	TCGTGCCTGATGACAAACAGGAGT	ATACTCGGTCTCGGCAGTGACTTT
MYH6	TCAGCTGGAGGCCAAAAGTAAAGGA	TTCTTGAGCTCTGAGCACTCGTCT
MYL2	TGTCCCTACCTTGTCTGTTAGCCA	ATTGGAACATGGCCTCTGGATGGA
MYL7	ACATCATCACCCATGGAGACGAGA	GCAACAGAGTTTATTGAGGTGCCC
NKX2.5	GCCGCCAACAACAACTTC	TACCAGGCTCGGATACCAT
TNNT2	AAGAAGAAGATTCTGGCTGAGAG	ACTTTCTGGTTATCGTTGATCCT
SLC27A6	CTTCTGTCATGGCTAACAGTTCT	AGGTTTCCGAGGTTGTCTTTTG
GAPDH	GGAGCGAGATCCCTCCAAAAT	GGCTGTTGTCATACTTCTCATGG

at different time points of gestation and created a FA metabolism gene set based on FA metabolism pathways annotated in the KEGG database (Supplementary Table 1), including FA supply, uptake, β-oxidation, other oxidation, and regulation.[1] To understand FA metabolism in the developing heart, we profiled FA metabolism-related genes in the human fetal heart. The dot plot in Figure 1A shows the expression percentages of these genes. Then, for genes with expression percentages above 50%, we generated a violin plot (Figure 1B). The results showed that FA metabolism exists in all cell types of human fetal hearts, suggesting that non-CMs also oxidize FAs for energy during heart development and maturation. Comparing the gene expressions among 5 W, 10 W, and 20 W fetal hearts, it was surprising that FA oxidation-related genes were generally downregulated over time. To determine whether the downregulation of FA oxidation was a programmed switch in energy substrate preference or a signal of reduced energy requirement, we investigated glycolysis metabolism in the human fetal heart (Supplementary Figure 3). We found that glycolysis was also downregulated over time, suggesting that substrate energy metabolism of the fetal heart at 20 W was decreased. As the embryonic heart formed and matured, it did not require as much energy as it did during the early stage of development. The changes in FA metabolism resulted from the reduction in energy requirements rather than from the alteration in the energy substrate usage strategy.

Unlike the downward trend of β-oxidation, some FA uptake- and transportation-related genes were upregulated in the later stages of cardiac maturation, revealing increased FA supply and uptake. Pearson correlation coefficients were then calculated to analyze the correlations between the five upregulated genes and other genes in the three types of CMs. Genes with a Pearson correlation coefficient greater than 0.6 are listed in Figure 1C-E. We performed KEGG enrichment analysis for the correlated genes and identified the top 20 enriched KEGG pathways (Figure 1F). These genes were found to be significantly involved in the PPAR pathway. As indicated in previous studies, PPAR is one of the key genes affecting the energy metabolism of CMs at the transcriptional level.[17,32] Therefore, the temporal expression differences of these genes during cardiac development may not directly affect β-oxidation but are related to the transcriptional regulation of energy metabolism.

Furthermore, we explored FA metabolism genes using a spatiotemporal transcriptome database.[33] Limited by the depth of the spatiotemporal transcriptome data, we found only five genes, namely, CD36 molecule (*CD36*), fatty acid binding protein 3 (*FABP3*), Acyl-CoA synthetase medium chain family member 3 (*ACSM3*), hydroxyacyl-CoA dehydrogenase trifunctional multienzyme complex subunit beta (*HADHB)*, and Enoyl-CoA delta isomerase 1 (*ECI1)* (Supplementary Figure 4). The expressions of *CD36* and *ACSM3* were found to be low from 4.5 W to 9 W, whereas *FABP3* was expressed broadly in the ventricular myocardium from 4.5 W to 9 W with high expression at 9 W, indicating that the expression patterns of genes involved in FA transport and activation had a time-specific pattern.

Fatty acid metabolism in human normal adult and failing hearts

To investigate FA metabolism in the adult human heart, we profiled FA metabolism-related genes in human normal adult and failing hearts using dot and violin plots. In contrast to the fetal heart, we found that FA metabolism, especially oxidation, was more specifically found in CMs from the adult heart (Figure 2A), indicating that non-CMs in the adult human heart did not need FAs as fuel.

During HF, the energy production of the whole heart was insufficient; however, we found that single CMs did not downregulate but instead upregulated FA metabolism to provide sufficient energy. There was almost no difference between the two HF types, caused by dilated cardiomyopathy and coronary heart disease, from the perspective of FA metabolism (Figure 2B). We found that FA metabolism was broadly upregulated in ventricular and atrial CMs in both the cHF and dHF groups; however, alteration of FA metabolism was lighter in AV CMs, suggesting that these CMs were different from ventricular and atrial CMs in terms of FA metabolism. FA oxidation in AV CMs was less affected than that in ventricular and atrial CMs, indicating a higher tolerance to stress in AV CMs.

Four genes [low density lipoprotein receptor, *CD36*, *FABP3*, and fatty acid binding protein 4 (*FABP4*)] were found to express FA metabolism-related genes, with percentages greater than 50% in non-CMs (Figure 2C). Al-

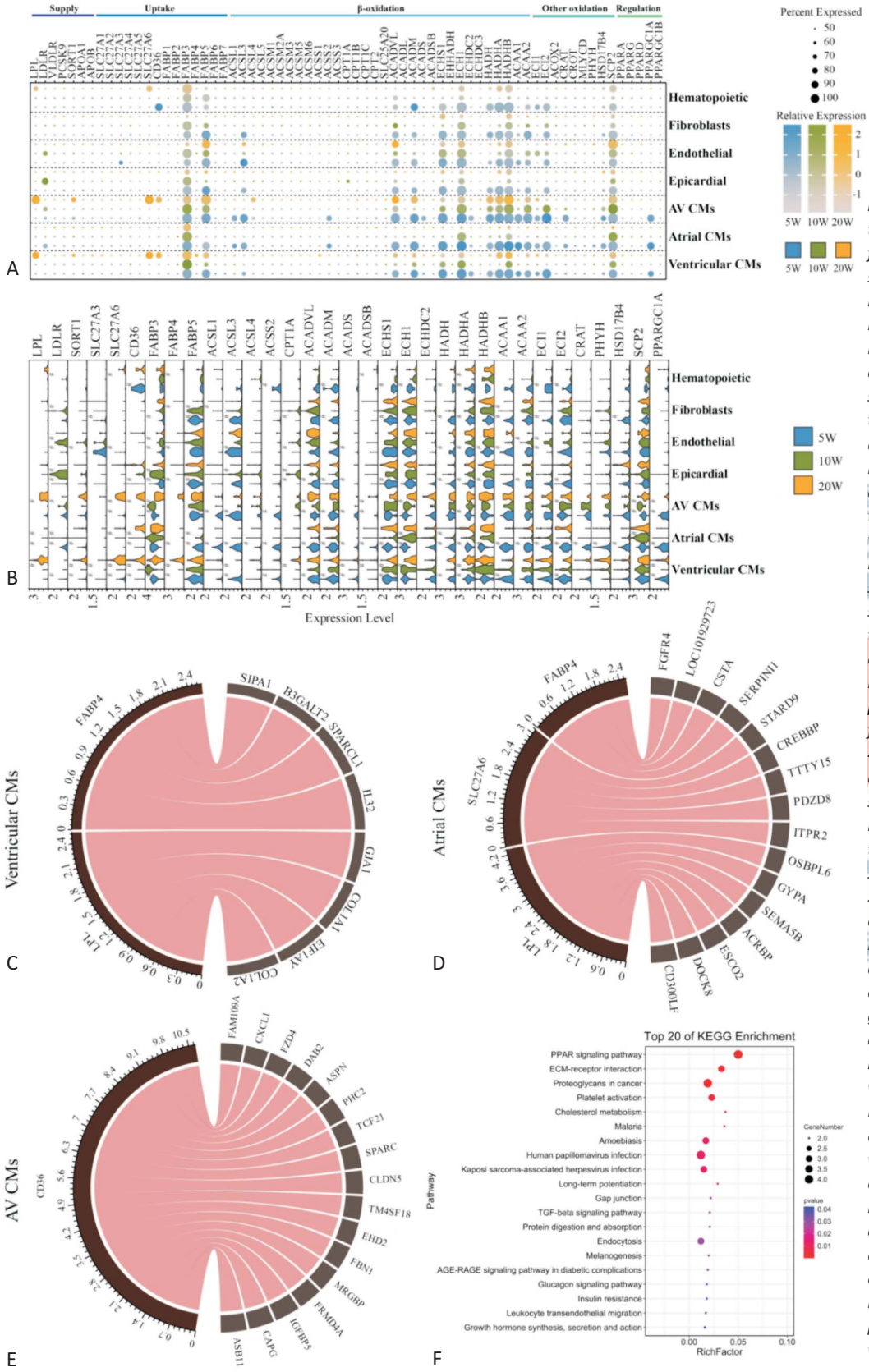

Figure 1. *Analysis of fatty acid metabolism in the fetal heart at single-cell resolution. (A) Dot plot showing the expression of selected fatty acid metabolism genes for seven cell clusters in fetal hearts. The size of the dots corresponds to the percentage of cardiac cells expressing the relevant gene per cell type, and their color represents the average expression level (cutoff = 50%). (B) Violin plot showing the expression of genes with expressed percentage greater than 50% in (A). (C) Chordal graph showing genes highly correlated with lipoprotein lipase (LPL) and fatty acid binding protein 4 (FABP4) in ventricular cardiomyocytes (CMs). Pearson coefficient was calculated to analyze correlation, and genes with Pearson correlation coefficient > 0.6 are listed. (D) Chordal graph showing genes highly correlated with LPL and FABP4 and SLC27A6 in atrial CMs. (E) Chordal graph showing genes highly correlated with CD36 molecule (CD36) in atrial and ventricular (AV) CMs. (F) Kyoto Encyclopedia of Genes and Genomes (KEGG) pathway enrichment analysis of highly correlated genes in fetal hearts. The color of the dots represents the adjusted p-value; the size of the dots represents the number of differentially expressed genes in the pathway.*

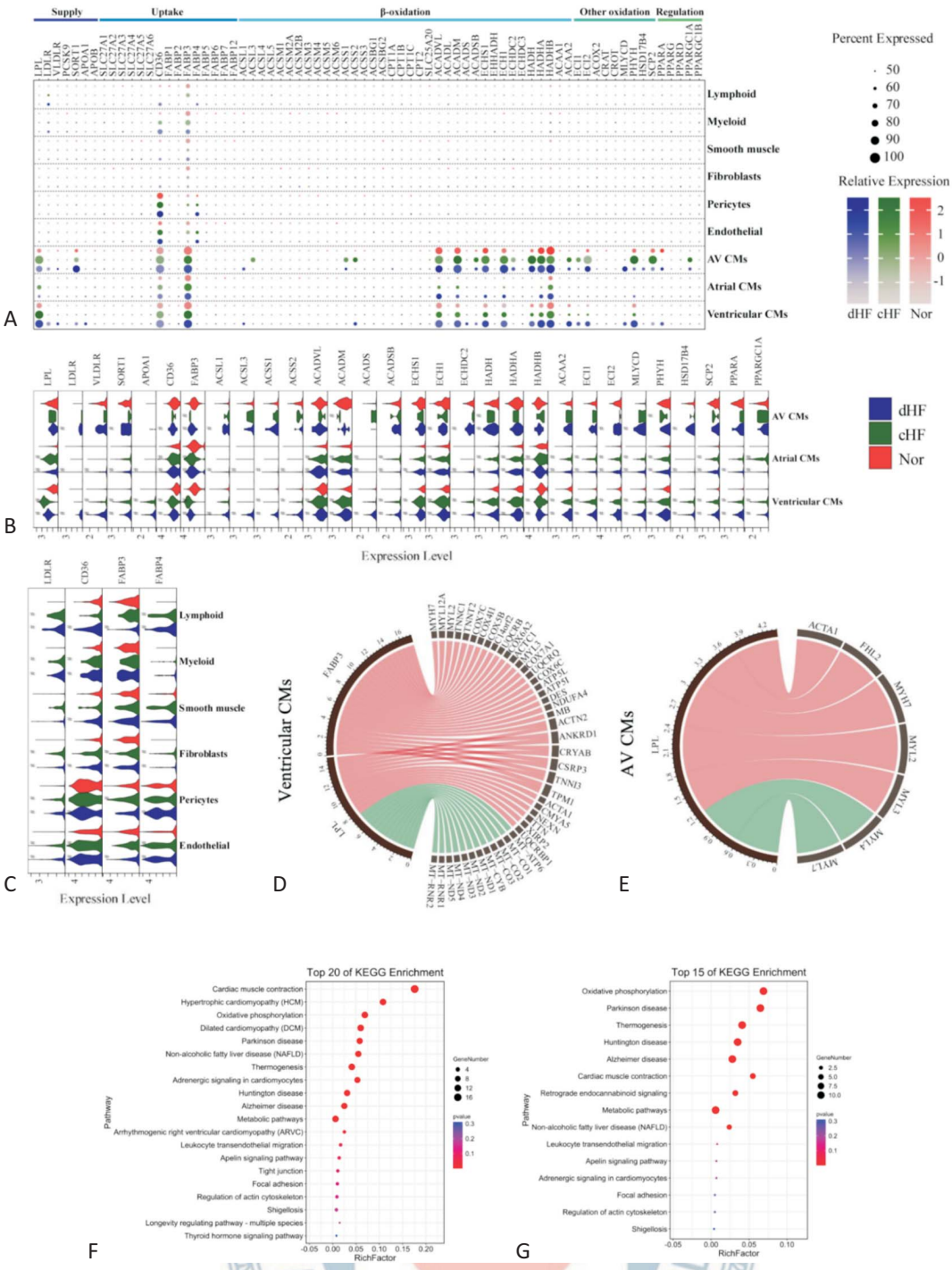

Figure 2. *Analysis of fatty acid metabolism in non-failing and failing adult hearts at the single-cell resolution. (A) Dot plot showing the expression of selected fatty acid metabolism genes for nine cell types and three groups of adult hearts (Nor, dHF, and cHF). The size of the dots corresponds to the percentage of cardiac cells expressing a certain gene per cell type, and its color represents the average expression level (cutoff = 50%). (B) Violin plot showing the expression of genes with the expressed percentage greater than 50% in Figure 3(A). (C) Violin plot showing the fatty acid metabolism genes expressed in non-cardiomyocytes with percentage greater than 50%. (D) Chordal graph depicting genes highly correlated with lipoprotein lipase (LPL) and FABP3 in ventricular cardiomyocytes (CMs). The Pearson coefficient was calculated to analyze correlation, and genes with Pearson correlation coefficient > 0.6 are listed. (E) Chordal graph depicting genes highly correlated with LPL in ventricular CMs (AV CMs). (F) KEGG pathway enrichment analysis of positively and (G) negatively correlated genes in failing hearts. The color of the dots represents the adjusted p-value; the size of the dots represents the number of differentially expressed genes in the pathway.*

though FA uptake was upregulated, oxidation-related genes were expressed at a low level.

We then calculated Pearson correlation coefficients between FA metabolism genes with expressed percentages above 50% and the other genes in CMs to identify the highly correlated genes (Pearson's correlation coefficient > 0.6) (Figure 2D-E). The top pathways enriched by KEGG analysis for the positively and negatively correlated genes are shown separately in Figure 2F-G.

The cardiac muscle contraction pathway was enriched mostly by positively correlated genes, confirming the compensatory strengthening at a single-cell level during HF. The oxidative phosphorylation pathway was enriched in negatively correlated genes, consistent with the reported disrupted oxidative metabolism in HF.[34]

SLC27A6 deficiency impaired cardiac gene expression and the morphology of hiPSC-CMs

In the scRNA-seq analysis, we observed a drastic change in the expression of *SLC27A6* along with maturation of the fetal heart (Figure 1A). SLC27A6, the predominant FATP isoform, is principally expressed in the heart on the sarcolemma and colocalizes with CD36.[24] SLC27A6 interacted with several FA metabolism-related genes, including CD36, FABP3 and FABP4 structurally and functionally (Supplementary Figure 5), and their expressions were found to be upregulated in the later stages of cardiac maturation, suggesting a special role in cardiac maturation. *SLC27A6* was also correlated with many important genes in fetal CMs (Figure 1D). However, the role of *SLC27A6* in heart maturation remains unclear.

To investigate how *SLC27A6* influences cardiac maturation, we differentiated human induced pluripotent stem cells into CMs and knocked down the expression of *SLC27A6* using *SLC27A6*-shRNA (KD-CMs) and scramble-shRNA [negative control (NC)-CMs] on day 9. First, we measured changes in the expressions of cardiac-related markers over time (Supplementary Figure 6), and the results suggested a successful time-dependent influence on CMs. We then measured the expression profile of *SLC27A6* mRNA during CM differentiation (Figure 3A), and the results revealed that its expression was relatively low and gradually increased as the CMs developed, consistent with our previous findings from single-cell data analysis (Figure 1A). The mRNA expression of *SLC27A6* increased gradually and reached a maximum, falling gradually instead of rising after that, indicating the temporal regulation of *SLC27A6* expression.

Furthermore, we examined how the expression patterns of cardiac-related markers differed between the NC-CM and KD-CM groups. The expression of *SLC27A6* in KD-CMs remained lower than that in NC-CMs (Figure 3B). Western blotting performed on the 28th day post-differentiation confirmed that its protein level was significantly downregulated (Figure 3C). To evaluate whether SLC27A6 affects the inherent gene expression of CMs, we analyzed the specific gene expression at different time points using quantitative real-time PCR. As shown in Figure 3D, compared with NC-CMs, the expression of the NK2 homeobox 5 (*NKX2.5*) gene, a cardiac progenitor cell marker, was significantly upregulated in KD-CMs; further, the gene required for cardiac contractile function (*TNNT2*) was downregulated, and the ratios of *MYH7*/Myosin heavy chain 6 (*MYH6*) and *MYL2*/*MYL7*, which indicate CM maturation, were found to be significantly decreased in KD-CMs. These results suggested that *SLC27A6* knockdown affected cardiac-specific gene expressions and led to an immature phenotype in CMs (Figure 3D).

Cell morphology is the most widely investigated and utilized factor in the measurement of CM maturation.[35] Representative immunostaining images of cTnT and DAPI staining demonstrated the influence of *SLC27A6* knockdown on CM morphology. Compared with NC-CMs, KD-CMs tended to have smaller areas and rounder shapes. Quantification of the average cellular size of KD-CMs revealed a substantial decrease (Figure 3E). An increase in punctate cTnT staining indicated a higher proportion of disordered myofilament structures (Figure 3E). Further, the percentage of cells with multiple nuclei, an indicator of CM maturation, was also greatly decreased (Figure 3F). These results suggested that a reduced expression of *SLC27A6* affected cardiac function negatively.

SLC27A6 deficiency attenuated Ca^{2+} handling activity and contractility of hiPSC-CMs

Calcium handling behavior is an important factor in determining CM maturation.[36] To investigate the effects of *SLC27A6* knockdown on the calcium handling behaviors of CMs, we measured spontaneous calcium transients using the fluorescent Ca^{2+} dye Cal-520 acetoxymethyl ester (Figure 4A). In contrast to NC-CMs, KD-CMs exhibited a shorter calcium transient amplitude, signifi-

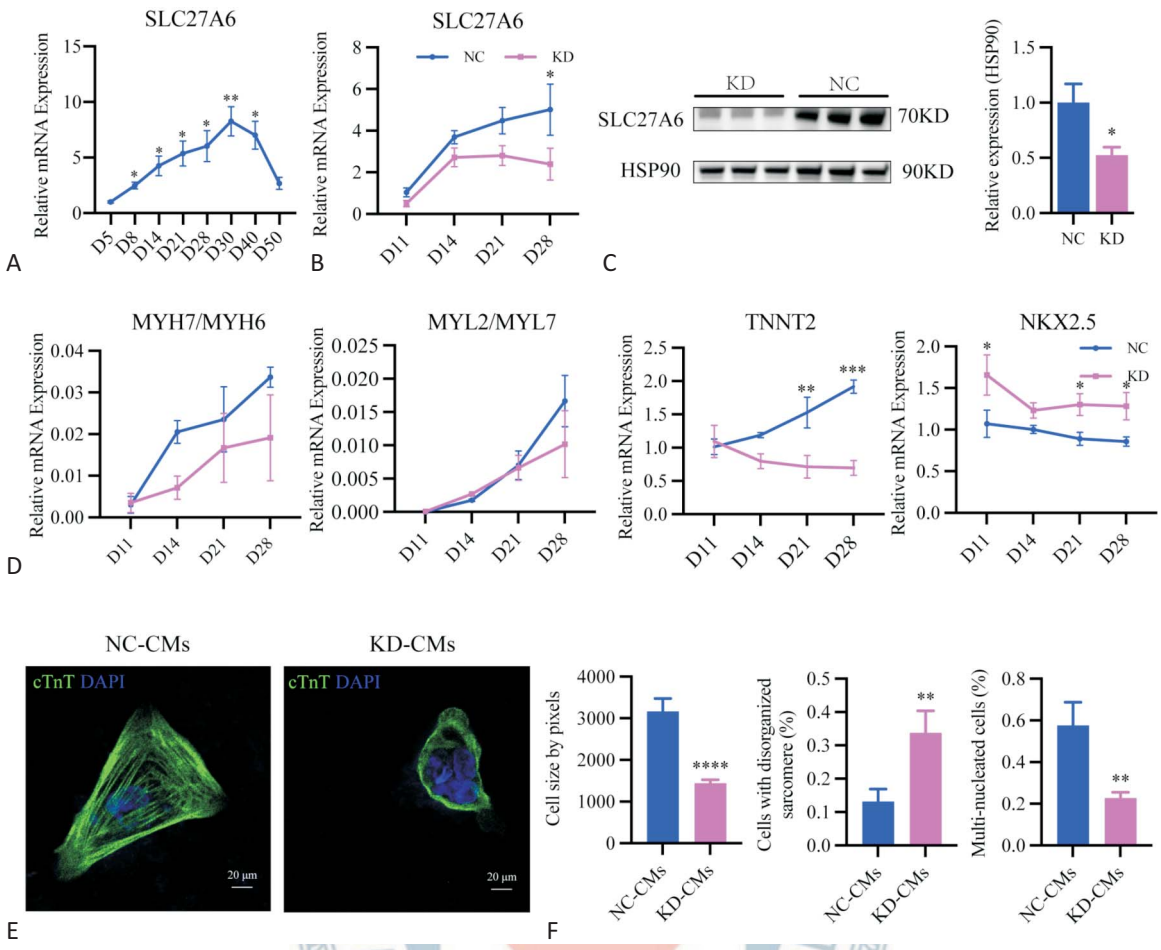

Figure 3. *Altered cardiac gene expression and morphology of hiPSC-CMs with SLC27A6 deficiency. (A) mRNA levels of SLC27A6 during the cardiomyocyte (CM) differentiation process. (B) mRNA levels of SLC27A6 in NC-CMs and KD-CMs. (C) Representative western blots showing the SLC27A6 levels in NC-CMs and KD-CMs. Quantification was performed using ImageJ. (D) Line graphs depicting the ratios of MYH7/MYH6 and MYL2/MYL7, and the mRNA levels of TNNT2 and NKX2.5 in NC-CMs and KD-CMs. (E) Representative images of immunofluorescence staining for cTnT (green) in NC-CMs and KD-CMs. Nuclei were stained with DAPI (blue) (original magnification ×40; scale bar = 20 μm). (F) Quantitation of cardiomyocyte area, percentage of cells with disorganized sarcomere and multi-nuclear cells, respectively. Data are presented as mean ± SEM of at least three independent experiments, as analyzed using the two-tailed Student's t test. * $p < 0.05$, ** $p < 0.01$, *** $p < 0.001$, **** $p < 0.0001$, relative to the control group. CM, cardiomyocyte; SEM, standard error of the mean; SLC27A6, solute carrier family 27 member 6.*

cantly prolonged transient duration of 50 s, increased peak to peak time, and longer decay time, which resulted in slower beating activity (Figure 4B). These variations indicated that the calcium-handling ability of CMs was weakened by *SLC27A6* deficiency.

Next, we explored whether *SLC27A6* knockdown affects changes in cardiac contractility by performing contractility assays on dissociated beating CMs on the 28th day post differentiation. Compared with NC-CMs, a slower beating frequency of KD-CMs was observed (Figure 4C), and contractility was significantly attenuated (Figure 4D), indicating that *SLC27A6* knockdown in CMs resulted in a reduction in contractile function.

DISCUSSION

Using scRNA-seq data analysis, our results indicate the heterogeneity of cell types in cardiac FA metabolism, reflecting the variances as well as links between single-cell metabolism and collective cardiac metabolism. Specifically, analysis of the fetal heart indicated a decline in total energy demand, other than an intermediate switch of energy substrates, which induced down-

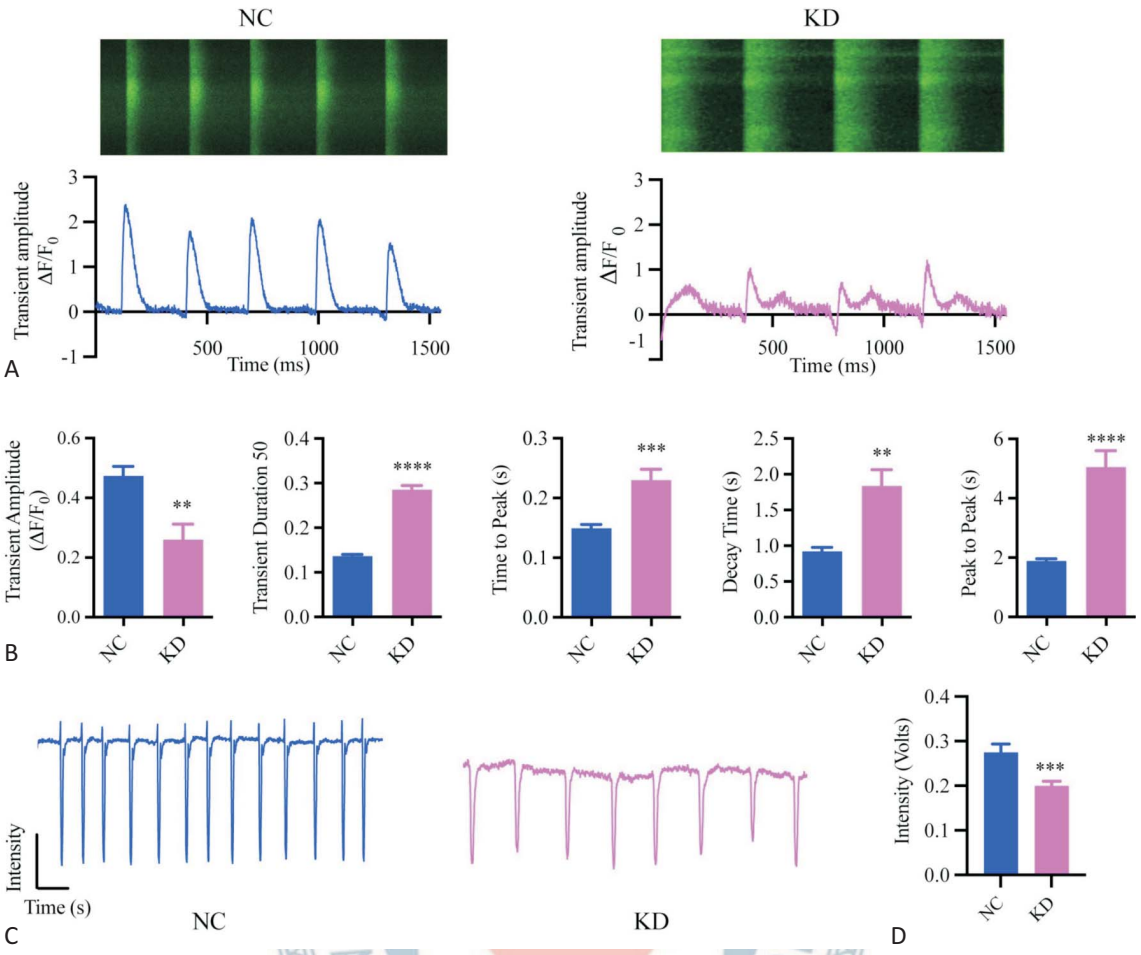

Figure 4. *Attenuated Ca^{2+} handling activity and contractility in hiPSC-CMs with SLC27A6 deficiency. (A) Representative line scan images depicting the calcium transients of single NC-CM and KD-CM. (B) Quantification of cardiomyocyte calcium imaging parameters for each group. (C) Representative images showing the contraction traces of two groups of hiPSC-CMs, recorded using the FelixGX detection system. (D) Quantification of contractility in single hiPSC-CMs from both groups. Data are presented as the mean ± SEM of at least three independent experiments, as analyzed using the two-tailed Student's t test. * p < 0.05, ** p < 0.01, *** p < 0.001, **** p < 0.0001, relative to the control group. CM, cardiomyocyte; hiPSC, human induced pluripotent stem cell; KD, SLC27A6 knockdown; NC, negative control; SEM, standard error of the mean; SLC27A6, solute carrier family 27 member 6.*

regulation of FA oxidation-related genes in the later period of cardiac maturation. Comparing the transcriptomic differences between non-failing and failing hearts, upregulation of FA metabolic genes within single CMs resulted from compensatory strengthening during HF in contrast to the total energy deficit. Notably, the novel role of *SLC27A6* in hiPSC-CM maturation was identified. We found that *SLC27A6* deficiency resulted in delayed CM development, abnormal morphology, and impaired contractile function compared with the negative control, suggesting that *SLC27A6* plays a critical role in CM maturation and physiological function.

In this study, we explored the critical role of FA metabolism in two important physiological/pathological processes, embryonic heart development and heart failure, at the single-cell level. Previous studies have shown that overall cardiac metabolism and FA metabolism decrease during HF,[37-39] accompanied by the downregulation of enzymes involved in FA oxidation.[40,41] However, our scRNA-seq results indicated that for single CMs, the FA metabolic level during heart failure was increased in a compensatory manner (Figure 2A-B). Thus, the overall decline in cardiometabolic levels was mainly induced by apoptosis and the consequent decrease in the number of CMs. Further, we also found that in CMs, the expressions of lipoprotein lipase (*LPL*) and *FABP3* were higher in both types of HF than in the non-failing hearts. Pearson correlation coefficient analysis was then performed

to identify the genes that were highly correlated with *LPL* and *FABP3*. KEGG analysis indicated that the positively correlated genes were enriched mostly in the cardiac muscle contraction pathway, verifying that individual CMs attempted to compensate for the generally reduced contractile function by activating the contraction pathway in HF. The negatively correlated genes were enriched in the oxidative phosphorylation pathway, representing poor mitochondrial organization and oxidative metabolism, which is consistent with the overall energy deficit and gradual decline in mitochondrial oxidative phosphorylation in patients with HF.[3]

In human embryonic hearts, we first analyzed both FA metabolic and glycolysis metabolic gene expression profiles to clarify that the decline in FA metabolism was caused by a reduction in overall energy demand, with no conflict in the switch between metabolic substrates. Among all of the genes related to FA metabolism, we found that those upregulated in the later stages of cardiac development and maturation all functioned to uptake and transport FAs. This metabolic phenotype could be partly attributed to the profile of energy substrates provided to the fetal heart. In fetal circulation, the level of maternal glucose is similar to the level of circulating glucose in newborns or adults, whereas the circulating level of maternal FAs is relatively low.[42] However, as the fetus develops, the maturing liver begins to provide nutrition for the whole body, including increasingly abundant lipoproteins, accounting for the increasing level of FA uptake and transport. Considering that increased FA uptake and transport were not consistent with the simultaneous decline in β-oxidation, these temporal upregulations could not be directly used for β-oxidation. In contrast, using Pearson correlation coefficient analysis and KEGG pathway analysis, we found genes that were highly correlated with these upregulated genes enriched in the PPAR pathway, one of the most important pathways modulating the energy metabolism and maturation of CMs at the transcriptional level.[17,32] Hence, these genes might be related to the transcriptional regulation of energy metabolism and CM maturation.

We focused on *SLC27A6* among these genes. SLC27A6 interacts with several FA metabolism-related proteins structurally and functionally, and we found that their gene expressions were upregulated in the later stages of cardiac maturation. Our analysis revealed that *SLC27A6* expression was maintained at a low level from the beginning and increased rapidly in the later stages of heart development, suggesting that it plays a crucial role in cardiac maturation. *SLC27A6* was also correlated with many important genes in fetal atrial CMs (Figure 1D); however, its role in heart maturation was unclear. A set of *in vitro* experiments was then conducted to define the function of *SLC27A6* in cardiac maturation.

First, the expression profile of *SLC27A6* was measured, and the results indicated that the temporal regulation of *SLC27A6* expression was related to specific developmental stages (Figure 3A). During heart maturation, a series of important cardiac maturation-related genes are programmed to be activated or repressed at specific developmental stages.[43] Rather than being expressed consistently at the same abundance, these genes are upregulated or downregulated at specific developmental stages for normal maturation.[44-46] *SLC27A6* was highly expressed at specific stages during cardiac maturation, suggesting that it was upregulated to meet developmental stage-specific needs and promote the development of the heart to a more mature state.

Next, we explored the effects of *SLC27A6* deficiency on iPSC-CMs at the developmental stage, during which *SLC27A6* should be highly expressed. Compared with contemporaneous NC-CMs, KD-CMs expressed lower levels of mature CM marker genes and showed abnormal morphology (Figure 3E-F). Calcium signals in KD-CMs were weaker and slower, in parallel with diminished contractile function (Figure 4). These differences suggested that after *SLC27A6* knockdown, the ability of CMs to handle calcium ions was weakened, requiring a longer time to release and recycle calcium ions, which significantly reduced the frequency of calcium transients. *SLC27A6*-deficient CMs may attenuate contractility through their reduced capacity to handle calcium ions. Generally, *SLC27A6* knockdown rendered KD-CMs developmentally delayed.

As SLC27A6 is the main isoform of FATPs expressed in the heart,[47] *SLC27A6* knockdown might directly damage the capacity to transport LCFAs in KD-CMs, which warrants further investigation. Moreover, FATPs function as LCFA transporters as well as ACSs to convert FAs into acyl-CoA thioesters.[19,21,22] FAs are taken in and prepared for subsequent metabolic processes by FATPs, and a concentration gradient of FAs can be maintained be-

tween extracellular and intracellular levels, facilitating the absorption of environmental FAs into the cytoplasm.[48-51] For KD-CMs, *SLC27A6* deficiency inhibited FA activation and attenuated the transmembrane gradient, thereby limiting the uptake and utilization of FAs. In mammalian embryos, cardiac maturation is accompanied by a general alteration from fetal metabolism to adult metabolism,[8] and the switch in energy substrate preference from carbohydrates to FAs is an important driver of cardiac maturation.[9] Impaired FA metabolism caused by *SLC27A6* deficiency might thus inhibit cardiac maturation by interfering with metabolic substrate transition. As discussed previously, *SLC27A6* may be related to the transcriptional regulation of CM metabolism and maturation, and its knockdown may affect energy metabolism at the transcriptional level.

As shown in Figure 3A, the mRNA expression of *SLC27A6* increased gradually and reached a maximum, then decreased along with the further maturation of CMs. As discussed, the upregulation of *SLC27A6* in 20 W fetal hearts may have contributed to the cardiac maturation by increasing FA transport and participating in transcriptional regulation. We hypothesize that the demand for FA supply in fully mature hearts tends to be stable and no longer increases as it does in partially mature hearts. Similarly, transcriptional regulation at specific developmental stages is no longer required. This was proved by *in vitro* experiments, in that *SLC27A6* showed a lower expression in fully mature CMs at later stages of development (Figure 3A), and according to our scRNA-seq analysis of normal adult hearts, this trend persisted into adulthood (Figure 2A).

Taken together, *SLC27A6* functions to encode FATP or as a transcriptional regulator, and *SLC27A6* deficiency inhibits the transition from fetal to adult metabolic patterns at specific developmental stages, thus restraining the normal maturation and function of KD-CMs (Central Illustration).

There are several possible limitations in this study. FA metabolism in single cells was studied only at the gene expression level, and further studies should investigate proteins and metabolites related to FA metabolism in different types of cells from a single-cell perspective. Meanwhile, results of *in vivo* experiments are still

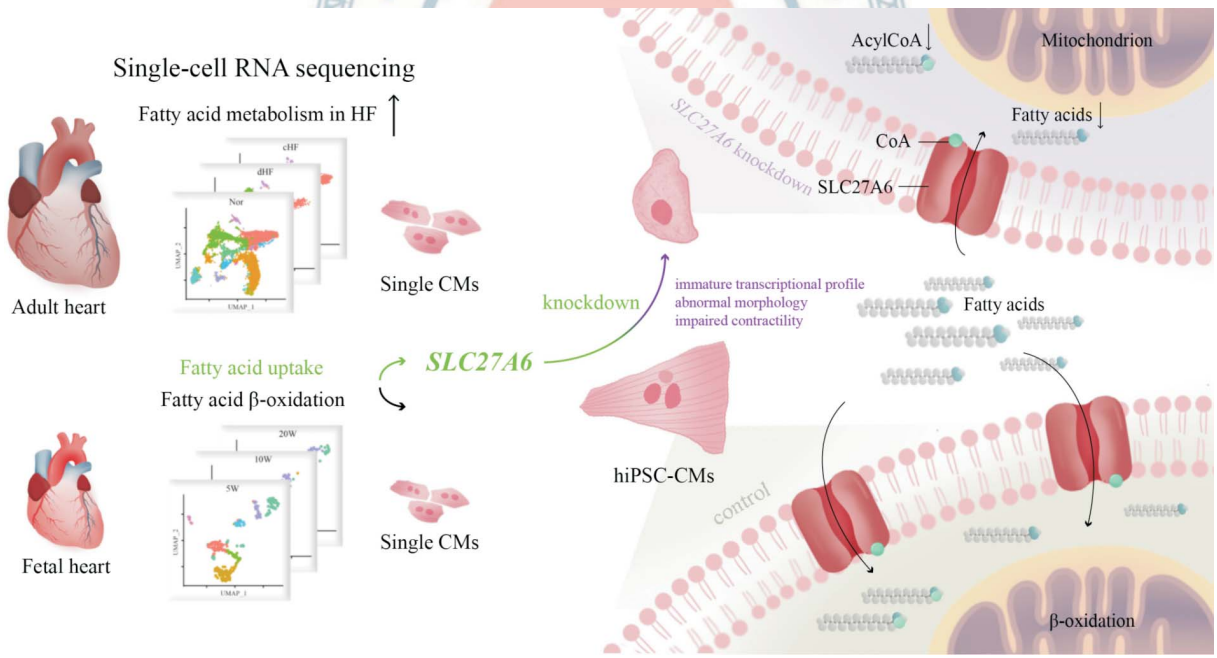

Central Illustration. *Schematic illustrations of the fatty acid (FA) metabolism in individual cardiac cells from fetal and failing hearts. The single-cell RNA sequencing (scRNA)-seq data analysis indicated the heterogeneity of cell types in cardiac FA metabolism, reflecting the compensatory increase of FA metabolism in individual cardiomyocytes (CMs) during heart failure (HF). In the later period of cardiac maturation, the FA oxidation-related genes downregulated while the genes functioning to uptake and transport Fas upregulated. Among these, the novel role of solute carrier family 27 member 6 (SLC27A6) in cardiac maturation was identified. SLC27A6 deficiency resulted in immature phenotypes in human induced pluripotent stem cell (hiPSC)-CMs, which could be attributed to impaired FA metabolic substrate transition and the transcriptional regulation of energy metabolism.*

needed to verify the importance of *SLC27A6* in cardiac maturation. Another limitation of this study is that we conducted experiments to validate the role of *SLC27A6* in prenatal fetal cardiac maturation, while insufficiently demonstrating its function in adult healthy and failing hearts. Although our scRNA-seq analysis revealed the FA metabolism of healthy adult CMs and HF CMs, further studies are needed to determine the expression of *SLC27A6* in normal and failing CMs, and corresponding *in vivo* experiments should be conducted to investigate the role of *SLC27A6* in adult healthy and failing hearts. Nevertheless, identification of the novel role of *SLC27A6* proved the feasibility of our protocol, and the present study provides new insights into FA metabolism in the heart.

Although *in vivo* experiments are required for further validation, and future studies are needed to elucidate the molecular mechanisms underlying the causal relationship between *SLC27A6* deficiency and delayed CM maturation, our study is the first to identify the critical role of this FATP-encoding gene in heart development and maturation. The findings of this study present the transcriptomic heterogeneity of energy metabolism among different types of cardiac cells as well as the cell-type-specific characteristics of FA metabolism in fetal and failing hearts. These results thus provide insights into the cellular mechanisms underlying FA metabolic alterations within individual cardiac cells and confirm the important role of the FATP6 encoding gene *SLC27A6* in cardiac maturation and physiological function. Demonstrating the causal relationship between a specific FA metabolic gene and the mature CM phenotype expands our understanding of FA metabolism in cardiac development and maturation. These discoveries indicate that scRNA-seq technology provides a new approach for the advanced understanding of cardiac metabolism, and that applying this technology could generate more intriguing insights into cellular transcriptome changes relevant to cardiac physiology and pathology.

CONCLUSIONS

Based on scRNA-seq analysis, we explored cardiac FA metabolism in individual cardiac cells, and our findings provide new insights into the cellular mechanisms underlying FA metabolic alterations in fetal and failing hearts. Experimental results confirmed that *SLC27A6* deficiency prevented the maturation of hiPSC-CMs. We hope this pilot transcriptomic analysis could advance the current understanding of FA metabolism during cardiac maturation and facilitate further exploration of cardiac physiology and pathology.

DECLARATION OF CONFLICT OF INTEREST

The authors declare no conflict of interest.

ACKNOWLEDGEMENTS

The authors would like to thank our lab colleagues for their support in the development of this article. The authors are also grateful to this article's reviewers and editor.

FUNDING SOURCES

This work was supported by the National Key R&D Program of China 2018YFC2000500/3 and National Natural Science Foundation of China (NSFC No.82070391, N.S.) and (NSFC No. 31900974, H.Y.).

REFERENCES

1. Lopaschuk GD, Ussher JR, Folmes CD, et al. Myocardial fatty acid metabolism in health and disease. *Physiol Rev* 2010;90:207-58.
2. Stanley WC, Recchia FA, Lopaschuk GD. Myocardial substrate metabolism in the normal and failing heart. *Physiol Rev* 2005; 85:1093-129.
3. Tuomainen T, Tavi P. The role of cardiac energy metabolism in cardiac hypertrophy and failure. *Exp Cell Res* 2017;360:12-8.
4. Neubauer S. The failing heart--an engine out of fuel. *N Engl J Med* 2007;356:1140-51.
5. Münzel T, Camici GG, Maack C, et al. Impact of oxidative stress on the heart and vasculature: part 2 of a 3-part series. *J Am Coll Cardiol* 2017;70:212-29.
6. Fisher DJ. Oxygenation and metabolism in the developing heart. *Semin Perinatol* 1984;8:217-25.
7. Lopaschuk GD, Spafford MA, Marsh DR. Glycolysis is predominant source of myocardial ATP production immediately after

birth. *Am J Physiol* 1991;261:H1698-705.
8. Lopaschuk GD, Jaswal JS. Energy metabolic phenotype of the cardiomyocyte during development, differentiation, and postnatal maturation. *J Cardiovasc Pharmacol* 2010;56:130-40.
9. Mills RJ, Titmarsh DM, Koenig X, et al. Functional screening in human cardiac organoids reveals a metabolic mechanism for cardiomyocyte cell cycle arrest. *Proc Natl Acad Sci U S A* 2017;114:E8372-81.
10. Hu D, Linders A, Yamak A, et al. Metabolic maturation of human pluripotent stem cell-derived cardiomyocytes by inhibition of HIF1α and LDHA. *Circ Res* 2018;123:1066-79.
11. Nakano H, Minami I, Braas D, et al. Glucose inhibits cardiac muscle maturation through nucleotide biosynthesis. *Elife* 2017;6:e29330.
12. Yang P, Chen X, Kaushal S, et al. High glucose suppresses embryonic stem cell differentiation into cardiomyocytes: high glucose inhibits ES cell cardiogenesis. *Stem Cell Res Ther* 2016;7:187.
13. Horikoshi Y, Yan Y, Terashvili M, et al. Fatty acid-treated induced pluripotent stem cell-derived human cardiomyocytes exhibit adult cardiomyocyte-like energy metabolism phenotypes. *Cells* 2019;8:1095.
14. Yang X, Rodriguez ML, Leonard A, et al. Fatty acids enhance the maturation of cardiomyocytes derived from human pluripotent stem cells. *Stem Cell Reports* 2019;13:657-68.
15. Ramachandra CJA, Mehta A, Wong P, et al. Fatty acid metabolism driven mitochondrial bioenergetics promotes advanced developmental phenotypes in human induced pluripotent stem cell derived cardiomyocytes. *Int J Cardiol* 2018;272:288-97.
16. Feyen DAM, McKeithan WL, Bruyneel AAN, et al. Metabolic maturation media improve physiological function of human iPSC-derived cardiomyocytes. *Cell Rep* 2020;32:107925.
17. Montessuit C, Palma T, Viglino C, et al. Effects of insulin-like growth factor-I on the maturation of metabolism in neonatal rat cardiomyocytes. *Pflugers Arch* 2006;452:380-6.
18. Poon E, Keung W, Liang Y, et al. Proteomic analysis of human pluripotent stem cell–derived, fetal, and adult ventricular cardiomyocytes reveals pathways crucial for cardiac metabolism and maturation. *Circ Cardiovasc Genet* 2015;8:427-36.
19. Houten SM, Wanders RJ. A general introduction to the biochemistry of mitochondrial fatty acid β-oxidation. *J Inherit Metab Dis* 2010;33:469-77.
20. Schrader M, Costello J, Godinho LF, et al. Peroxisome-mitochondria interplay and disease. *J Inherit Metab Dis* 2015;38:681-702.
21. Anderson CM, Stahl A. SLC27 fatty acid transport proteins. *Mol Aspects Med* 2013;34:516-28.
22. Black PN, DiRusso CC. Yeast acyl-CoA synthetases at the crossroads of fatty acid metabolism and regulation. *Biochim Biophys Acta* 2007;1771:286-98.
23. Doege H, Stahl A. Protein-mediated fatty acid uptake: novel insights from in vivo models. *Physiology (Bethesda)* 2006;21:259-68.
24. Gimeno RE, Ortegon AM, Patel S, et al. Characterization of a heart-specific fatty acid transport protein. *J Biol Chem* 2003;278:16039-44.
25. Auinger A, Helwig U, Pfeuffer M, et al. A variant in the heart-specific fatty acid transport protein 6 is associated with lower fasting and postprandial TAG, blood pressure and left ventricular hypertrophy. *Br J Nutr* 2012;107:1422-8.
26. Irvin MR, Aggarwal P, Claas SA, et al. Whole-exome sequencing and hiPSC cardiomyocyte models identify MYRIP, TRAPPC11, and SLC27A6 of potential importance to left ventricular hypertrophy in an African ancestry population. *Front Genet* 2021;12:588452.
27. Molenaar B, van Rooij E. Single-cell sequencing of the mammalian heart. *Circ Res* 2018;123:1033-5.
28. Litviňuková M, Talavera-López C, Maatz H, et al. Cells of the adult human heart. *Nature* 2020;588:466-72.
29. Zhang X, Lan Y, Xu J, et al. CellMarker: a manually curated resource of cell markers in human and mouse. *Nucleic Acids Res* 2019;47:D721-8.
30. Cui Y, Zheng Y, Liu X, et al. Single-cell transcriptome analysis maps the developmental track of the human heart. *Cell Rep* 2019;26:1934-50.e5.
31. Wang Q, Yang H, Bai A, et al. Functional engineered human cardiac patches prepared from nature's platform improve heart function after acute myocardial infarction. *Biomaterials* 2016;105:52-65.
32. Montaigne D, Butruille L, Staels B. PPAR control of metabolism and cardiovascular functions. *Nat Rev Cardiol* 2021;18:809-23.
33. Asp M, Giacomello S, Larsson L, et al. A spatiotemporal organ-wide gene expression and cell atlas of the developing human heart. *Cell* 2019;179:1647-60.e19.
34. Schwemmlein J, Maack C, Bertero E. Mitochondria as therapeutic targets in heart failure. *Curr Heart Fail Rep* 2022.
35. Spach MS, Heidlage JF, Barr RC, et al. Cell size and communication: role in structural and electrical development and remodeling of the heart. *Heart Rhythm* 2004;1:500-15.
36. Ronaldson-Bouchard K, Ma SP, Yeager K, et al. Advanced maturation of human cardiac tissue grown from pluripotent stem cells. *Nature* 2018;556:239-43.
37. Abozguia K, Shivu GN, Ahmed I, et al. The heart metabolism: pathophysiological aspects in ischaemia and heart failure. *Curr Pharm Des* 2009;15:827-35.
38. Ventura-Clapier R, Garnier A, Veksler V. Energy metabolism in heart failure. *J Physiol* 2004;555:1-13.
39. Tuunanen H, Ukkonen H, Knuuti J. Myocardial fatty acid metabolism and cardiac performance in heart failure. *Curr Cardiol Rep* 2008;10:142-8.
40. Sack MN, Rader TA, Park S, et al. Fatty acid oxidation enzyme gene expression is downregulated in the failing heart. *Circulation* 1996;94:2837-42.
41. Razeghi P, Young ME, Alcorn JL, et al. Metabolic gene expression in fetal and failing human heart. *Circulation* 2001;104:2923-31.
42. Girard J, Ferré P, Pégorier JP, et al. Adaptations of glucose and fatty acid metabolism during perinatal period and suckling-weaning transition. *Physiol Rev* 1992;72:507-62.
43. DeLaughter DM, Bick AG, Wakimoto H, et al. Single-cell resolu-

tion of temporal gene expression during heart development. *Dev Cell* 2016;39:480-90.
44. Lints TJ, Parsons LM, Hartley L, et al. Nkx-2.5: a novel murine homeobox gene expressed in early heart progenitor cells and their myogenic descendants. *Development* 1993;119:419-31.
45. Bu L, Jiang X, Martin-Puig S, et al. Human ISL1 heart progenitors generate diverse multipotent cardiovascular cell lineages. *Nature* 2009;460:113-7.
46. Qyang Y, Martin-Puig S, Chiravuri M, et al. The renewal and differentiation of Isl1+ cardiovascular progenitors are controlled by a Wnt/beta-catenin pathway. *Cell Stem Cell* 2007;1:165-79.
47. Longo N, Frigeni M, Pasquali M. Carnitine transport and fatty acid oxidation. *Biochim Biophys Acta* 2016;1863:2422-35.
48. Cooper DE, Young PA, Klett EL, et al. Physiological consequences of compartmentalized acyl-CoA metabolism. *J Biol Chem* 2015; 290:20023-31.
49. Black PN, DiRusso CC. Vectorial acylation: linking fatty acid transport and activation to metabolic trafficking. *Novartis Found Symp* 2007;286:127-38; discussion 38-41, 62-3, 96-203.
50. Arias-Barrau E, Dirusso CC, Black PN. Methods to monitor fatty acid transport proceeding through vectorial acylation. *Methods Mol Biol* 2009;580:233-49.
51. Tong F, Black PN, Coleman RA, et al. Fatty acid transport by vectorial acylation in mammals: roles played by different isoforms of rat long-chain acyl-CoA synthetases. *Arch Biochem Biophys* 2006; 447:46-52.

SUPPLEMENTARY MATERIALS

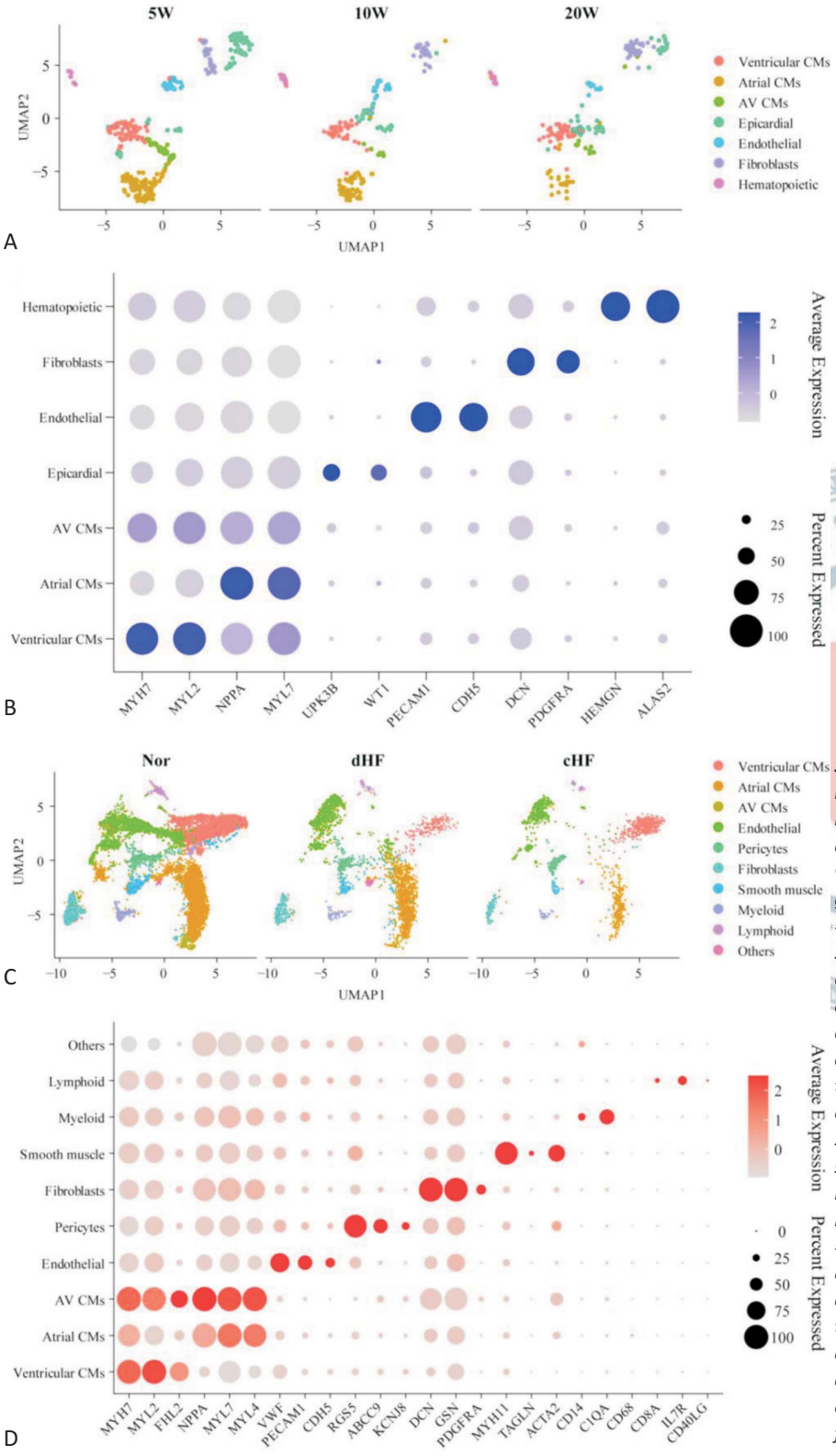

Supplementary Figure 1. *Clustering and identification of cell types in fetal and adult hearts. (A) UMAP projection of 1528 human cardiac cells from fetal hearts showing seven clusters, annotated based on marker genes (cell numbers from the left to right: n = 766 for 5 W, n = 384 for 10 W, n = 378 for 20 W). (B) Dot plot showing the expression of selected marker genes for the seven cell clusters in fetal hearts. The size of the dots corresponds to the percentage of cardiac cells expressing the certain gene per cell type, and their color represents the average expression level. (C) UMAP projection of 27550 human cardiac cells from adult hearts showing 10 clusters, annotated based on marker genes (cell numbers from left to right: n = 19364 for Nor, n = 5386 for dHF, n = 2800 for cHF). (D) Dot plot showing the expression of selected marker genes for 10 cell clusters from adult hearts. The size of the dots corresponds to the percentage of cardiac cells expressing the certain gene per cell type, and their color represents the average expression level. UMAP, uniform manifold approximation and projection.*

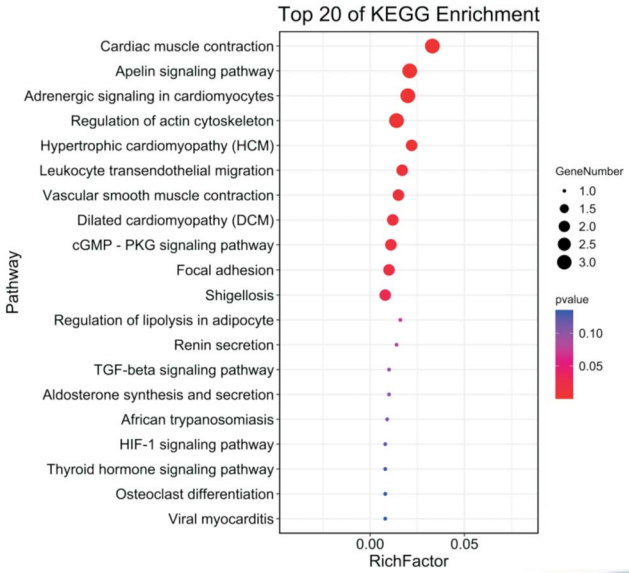

Supplementary Figure 2. *Kyoto Encyclopedia of Genes and Genomes (KEGG) pathway enrichment analysis of marker genes in the atrial and ventricular cardiomyocytes (AV CMs) cluster. KEGG pathway enrichment analysis of the marker genes of the AV CMs cluster. The color of the dots represents the adjusted p-value, and the size of the dots represents the number of differentially expressed genes in the pathway.*

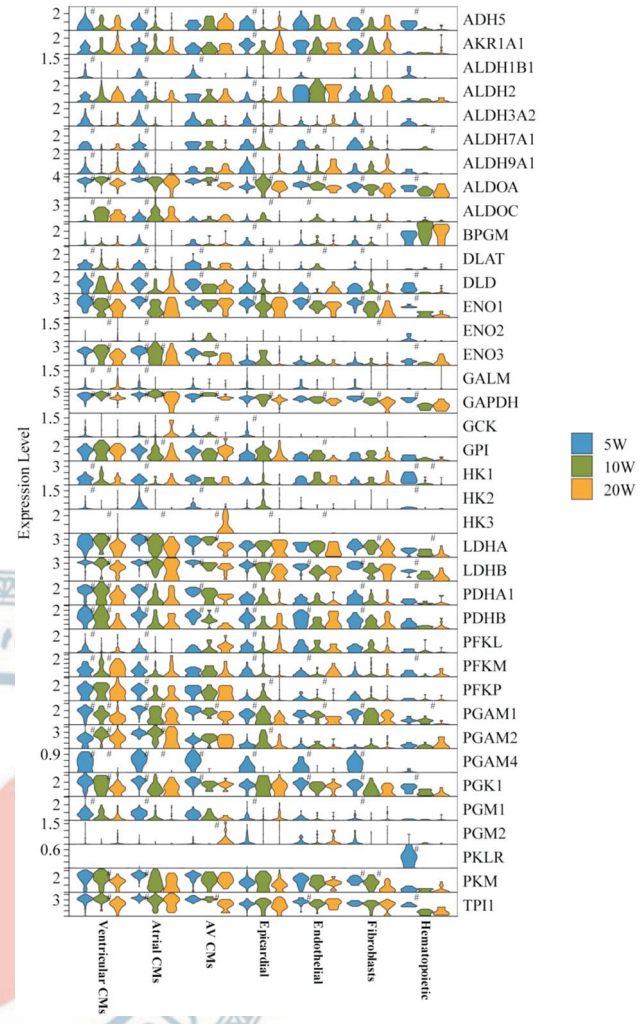

Supplementary Figure 3. *Analysis of glycolysis metabolism in the fetal heart at a single-cell resolution. Violin plot showing the expression of selected glycolysis metabolism genes for seven cell clusters from fetal hearts.*

Supplementary Table 1. Fatty acid metabolism gene set

Fatty acids uptake	*SLC27A1, SLC27A2, SLC27A3, SLC27A4, SLC27A5, SLC27A6, CD36, FABP1, FABP2, FABP3, FABP4, FABP5, FABP6, FABP7, FABP12*
Fatty acids oxidation	
β-oxidation	*ACSL1, ACSL3, ACSL4, ACSL5, ACSM1, ACSM2A, ACSM2B, ACSM3, ACSM4, ACSM5, ACSM6, ACSS1, ACSS2, ACSS3, ACSBG1, ACSBG2, CPT1A, CPT1B, CPT1C, CPT2, SLC25A20, ACADVL, ACADL, ACADM, ACADS, ACADSB, ECHS1, EHHADH, ECH1, ECHDC2, ECHDC3, HADH, HADHA, HADHB, ACAA1, ACAA2*
Other oxidation	*ECI1, ECI2, ACOX2, CRAT, CROT, MLYCD, PHYH, HSD17B4, SCP2*
Fatty acids biosynthesis	*FASN, ACACA, ACACB, ELOVL1, ELOVL2, ELOVL3, ELOVL4, ELOVL5, ELOVL6, ELOVL7, TECR, ACOT1, ACOT7, THEM4, THEM5, PPT1, PPT2, HSD17B12, BAAT, SCD, FADS1, FADS2*

This table shows a list of fatty acid metabolism genes based on the Kyoto Encyclopedia of Genes and Genomes (KEGG) database.

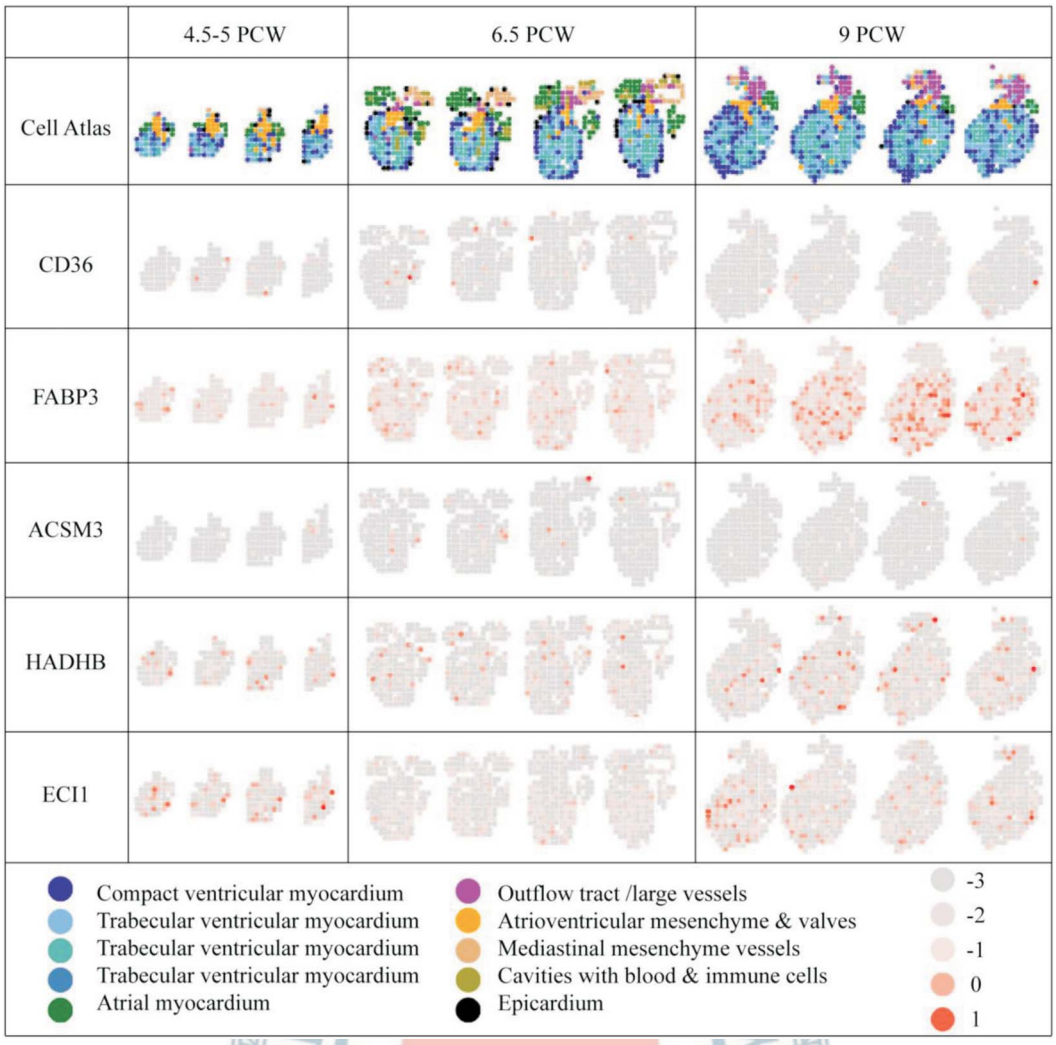

Supplementary Figure 4. *Expression of six fatty acid metabolism genes in a spatiotemporal transcriptome database. Different spatiotemporal gene expressions of CD36 molecule (CD36), fatty acid binding protein 3 (FABP3), Acyl-CoA synthetase medium chain family member 3 (ACSM3), hydroxyacyl-CoA dehydrogenase trifunctional multienzyme complex subunit beta (HADHB), and Enoyl-CoA delta isomerase 1 (ECI1) in fetal hearts. PCW, post-conception weeks.*

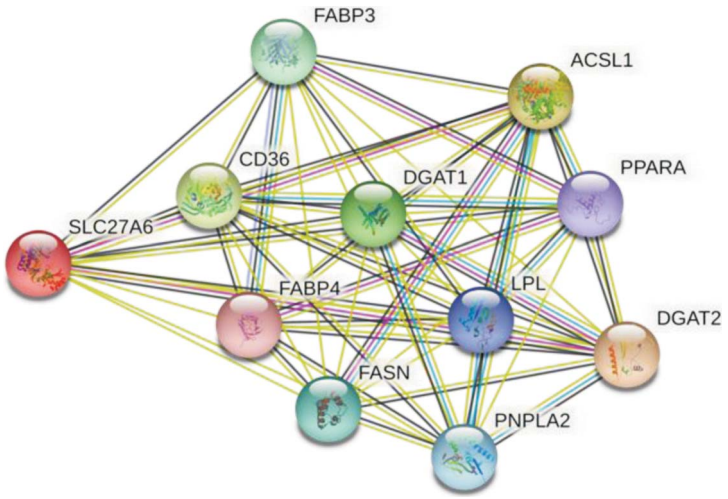

Supplementary Figure 5. *Interactions between SLC27A6 and CD36, FABP3, FABP4. The SLC27A6 protein-associated network was analyzed via STRING database.*

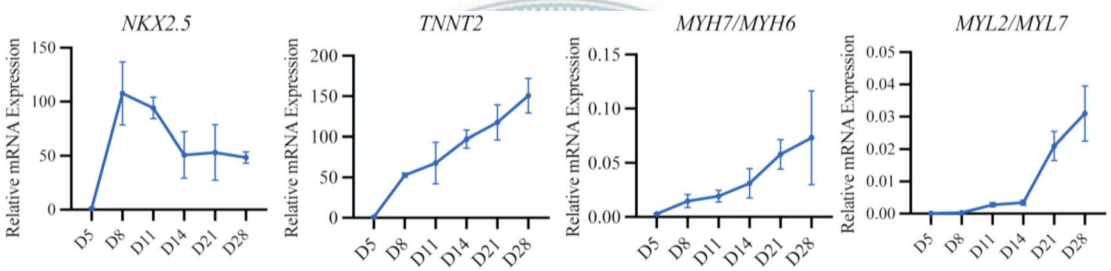

Supplementary Figure 6. *Expression pattern of key markers regulating in vitro cardiomyocyte directed differentiation. Line graphs depicting the mRNA levels of key markers at various stages of cardiomyocyte differentiation. Data are presented as the mean ± SEM of at least three independent experiments relative to the control group. NKX2.5, NK2 homeobox 5; SEM, standard error of the mean; TNNT2, cardiac troponin T (gene).*